Energy Materials

Supplementary Materials

Asymmetric carbazole-based self-assembled monolayers enable simultaneous efficiency and stability enhancement in organic solar cells

Yangyang Yu[1], Xin Hong[2], Yuan Li[2], Zhengfei Wang[2], Feiyu Kang[2], Zhiwei Jiao[1,*], Guodan Wei[2,*]

[1]College of Science, China Jiliang University, Hangzhou 310018, Zhejiang, China.
[2]Institute of Materials Research, Tsinghua Shenzhen International Graduate School, Tsinghua University, Shenzhen 518000, Guangdong, China.

Correspondence to: Prof. Guodan Wei, Institute of Materials Research, Tsinghua Shenzhen International Graduate School, Tsinghua University, Shenzhen 518000, Guangdong, China. E-mail: weiguodan@sz.tsinghua.edu.cn; Prof. Zhiwei Jiao, College of Science, China Jiliang University, Hangzhou 310018, Zhejiang, China. E-mail: jzwgj@163.com

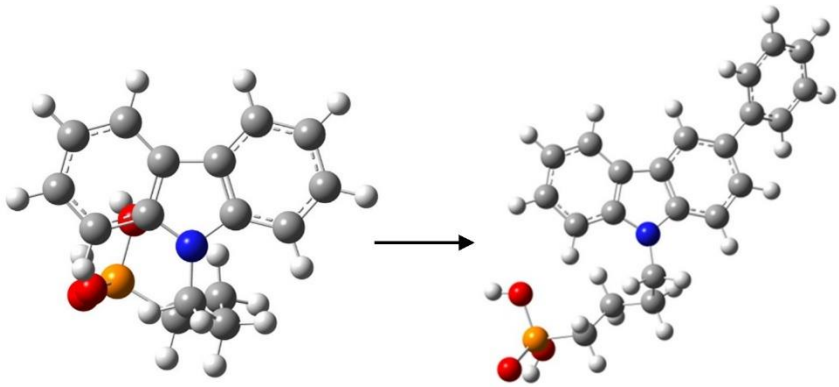

Supplementary Figure 1. Calculated molecular structures (front views) of 4PACz and P-4PACz.

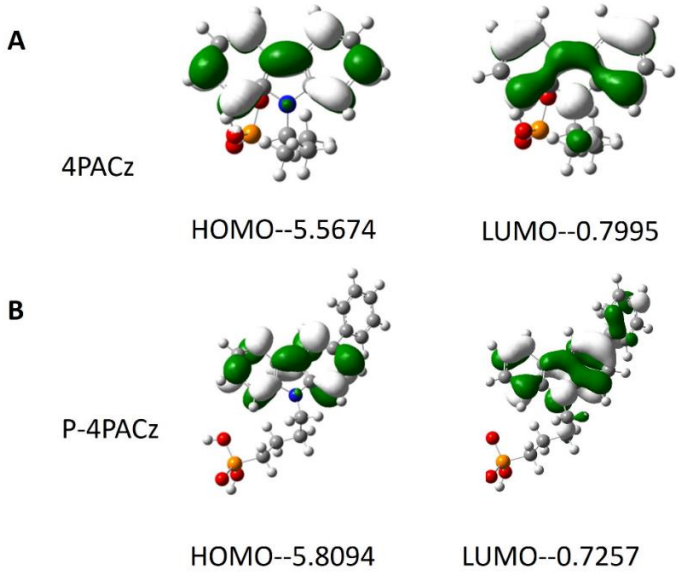

Supplementary Figure 2. HOMO/LUMO levels of 4PACz and P-4PACz.

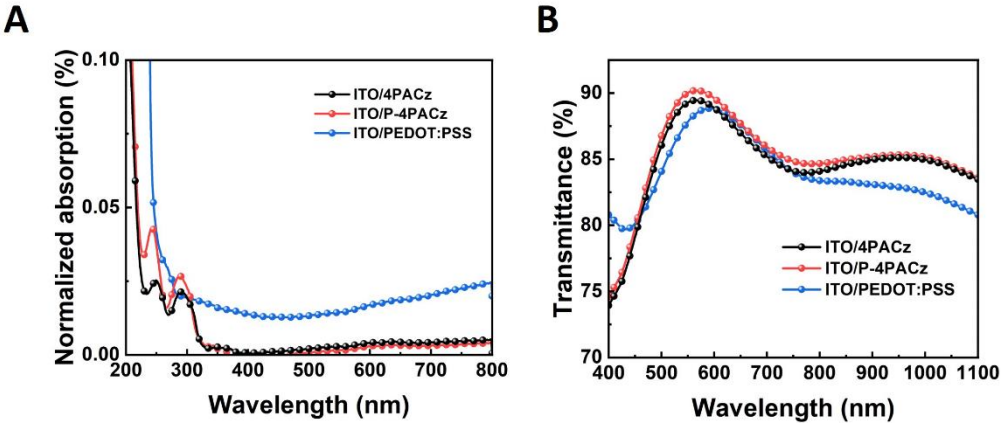

Supplementary Figure 3. (A) UV–vis absorption spectra of 4PACz and P-4PACz. (B) Transmittance of 4PACz, P-4PACz, and PEDOT:PSS on ITO/glass.

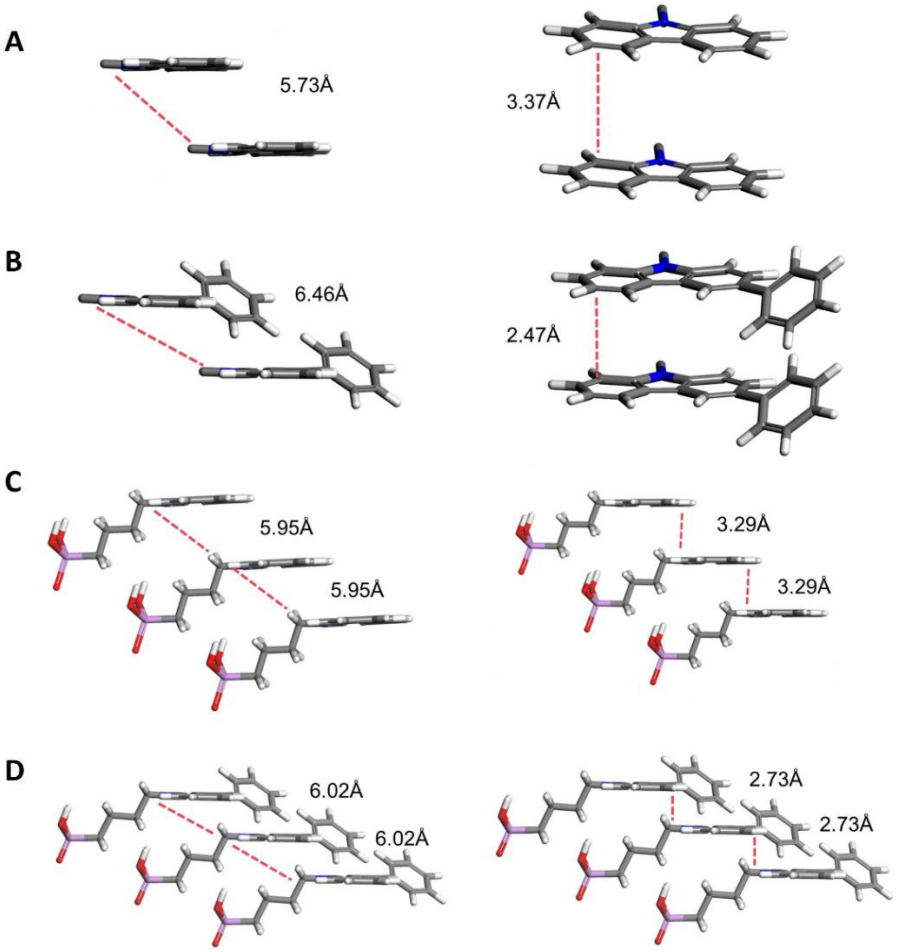

Supplementary Figure 4. The molecular packing patterns observed in single crystals: (A) pristine carbazole and (B) 3-phenyl-9H-carbazole (retrieved from the CCDC database), (C) 4PACz and (D) P-4PACz.

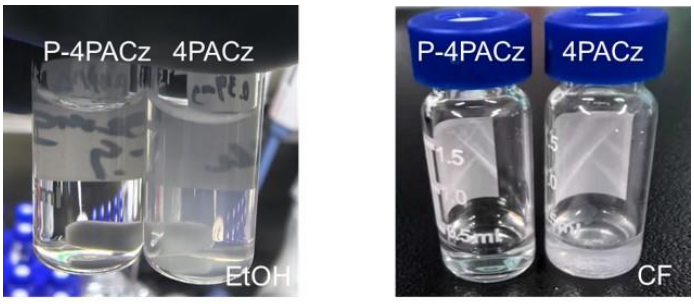

Supplementary Figure 5. Solubility comparison of 4PACz and P-4PACz in (left) ethanol and (right) chloroform at a concentration of 0.5 mg/mL.

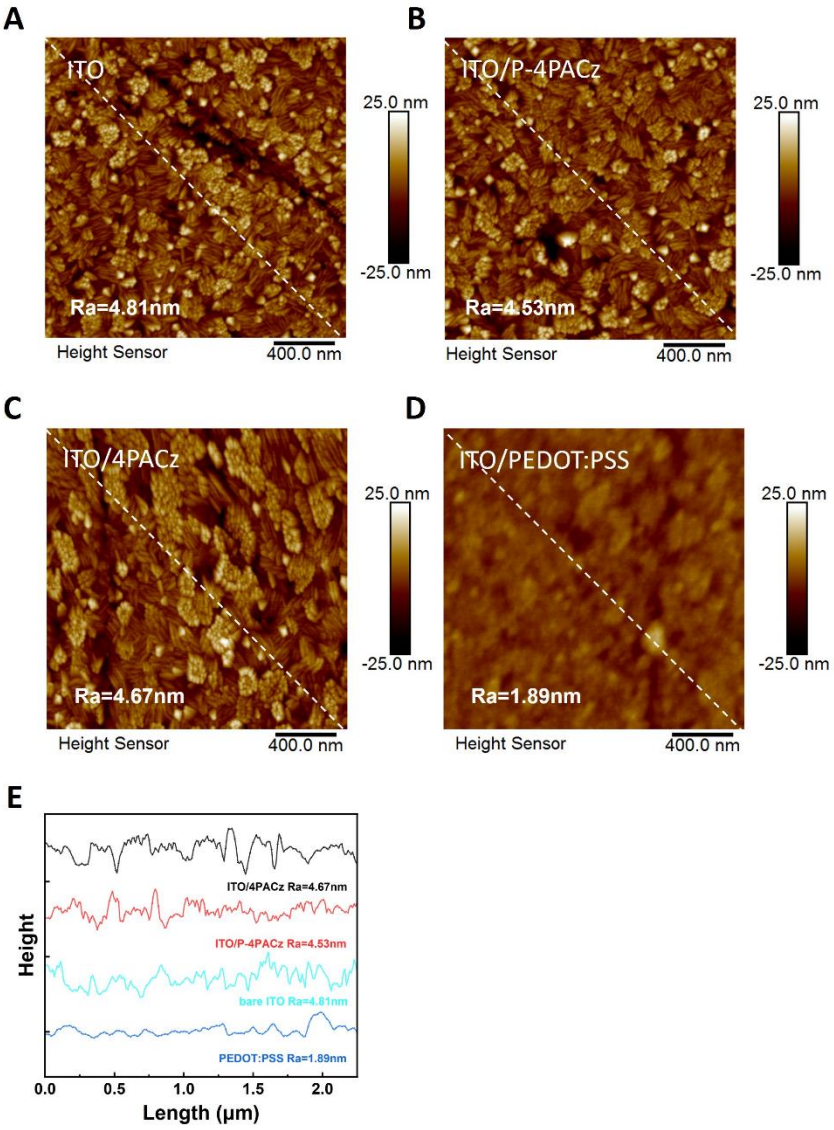

Supplementary Figure 6. AFM images of: (A) ITO; (B) 4PACz; (C) P-4PACz; (D) PEDOT:PSS on ITO; E, Height images of the AFM sectional diagram corresponding to ITO/HTLs.

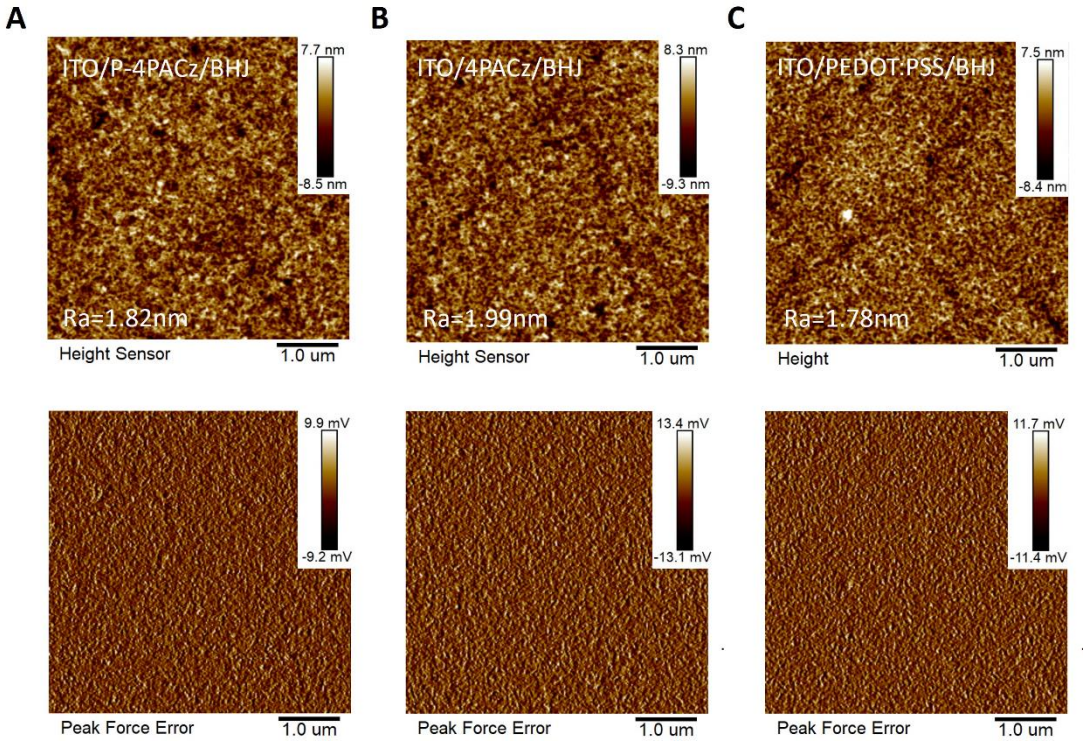

Supplementary Figure 7. AFM images of: (A) ITO/P-4PACz/BHJ; (B) ITO/4PACz/BHJ; (C) ITO/PEDOT:PSS/BHJ.

Supplementary Figure 8. Formamide contact angles on: bare ITO; ITO/4PACz; ITO/P-4PACz; (D) ITO/PEDOT:PSS.

Supplementary Figure 9. H_2O contact angles on: bare ITO; ITO/4PACz; ITO/P-4PACz; ITO/PEDOT:PSS.

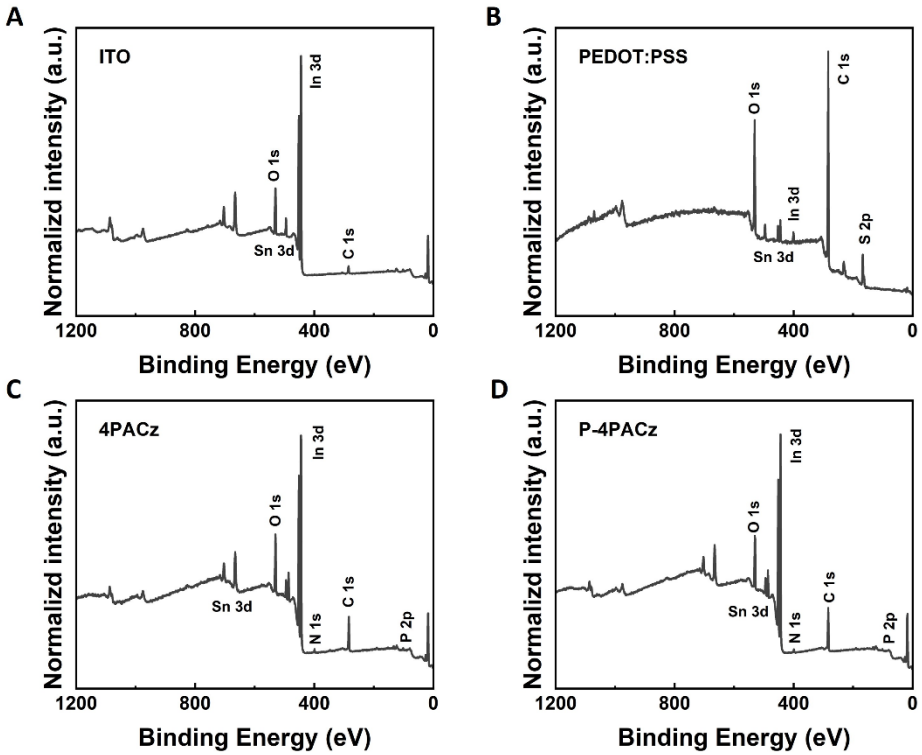

Supplementary Figure 10. XPS survey spectra of: (A) bare ITO (reference); (B) ITO/PEDOT:PSS; (C) ITO/4PACz; (D) ITO/P-4PACz.

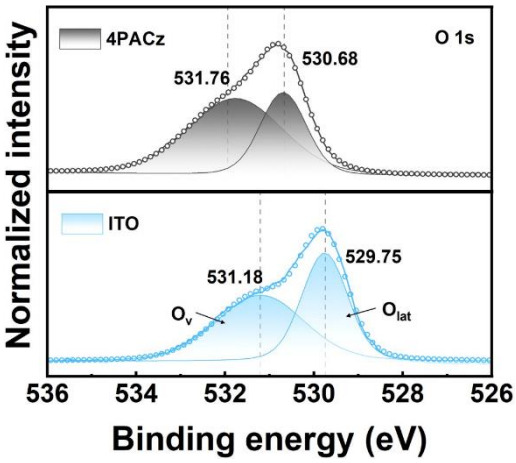

Supplementary Figure 11. O 1s XPS spectra of bare ITO and ITO/4PACz.

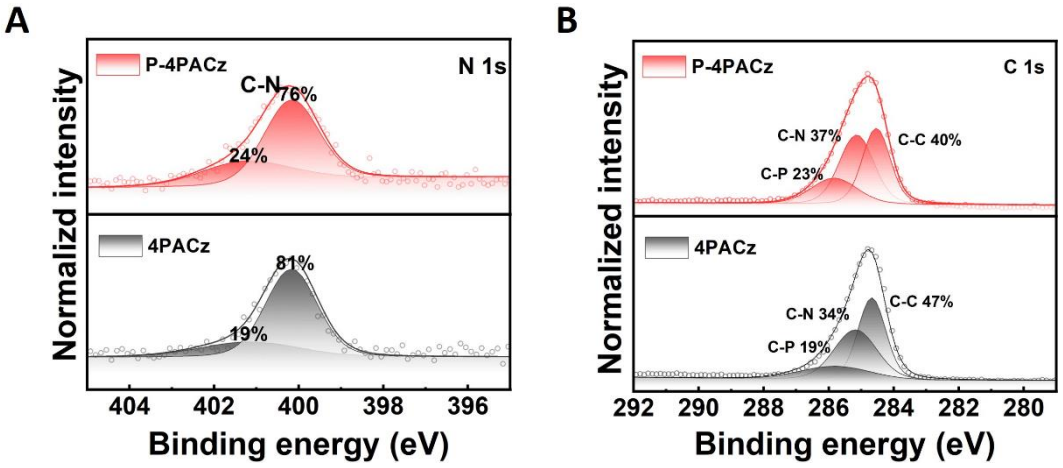

Supplementary Figure 12. (A) N 1s and (B) C 1s XPS spectra of bare ITO, ITO/4PACz, and ITO/P-4PACz.

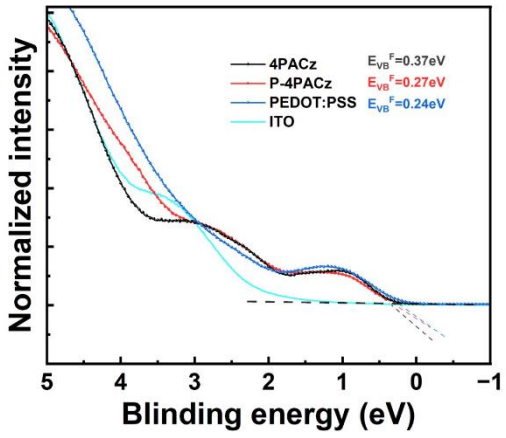

Supplementary Figure 13. ITO, 4PACz, P-4PACz, and PEDOT:PSS Fermi edge region.

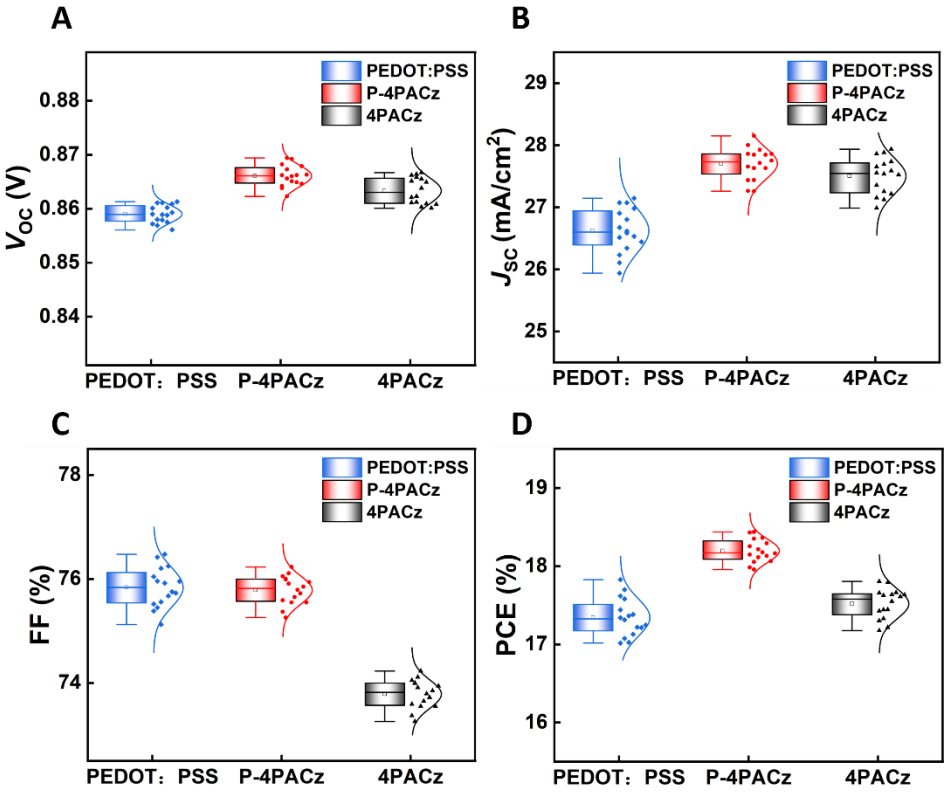

Supplementary Figure 14. Statistical (A) V_{OC}, (B) J_{SC}, (C) FF, (D) PCE of OSCs on 4PACz, P-4PACz, and PEDOT:PSS substrates.

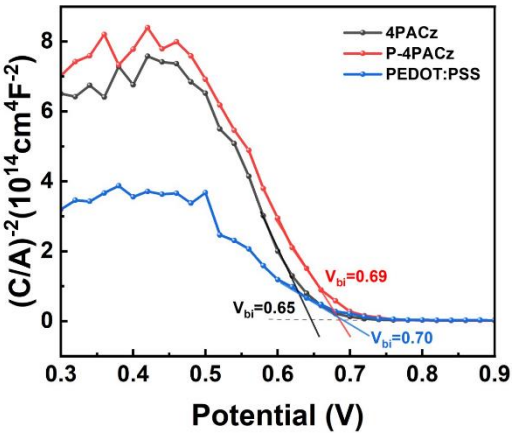

Supplementary Figure 15. Mott-Schottky (C^{-2}–V) curves for ITO/4PACz, ITO/P-4PACz, and ITO/PEDOT:PSS devices.

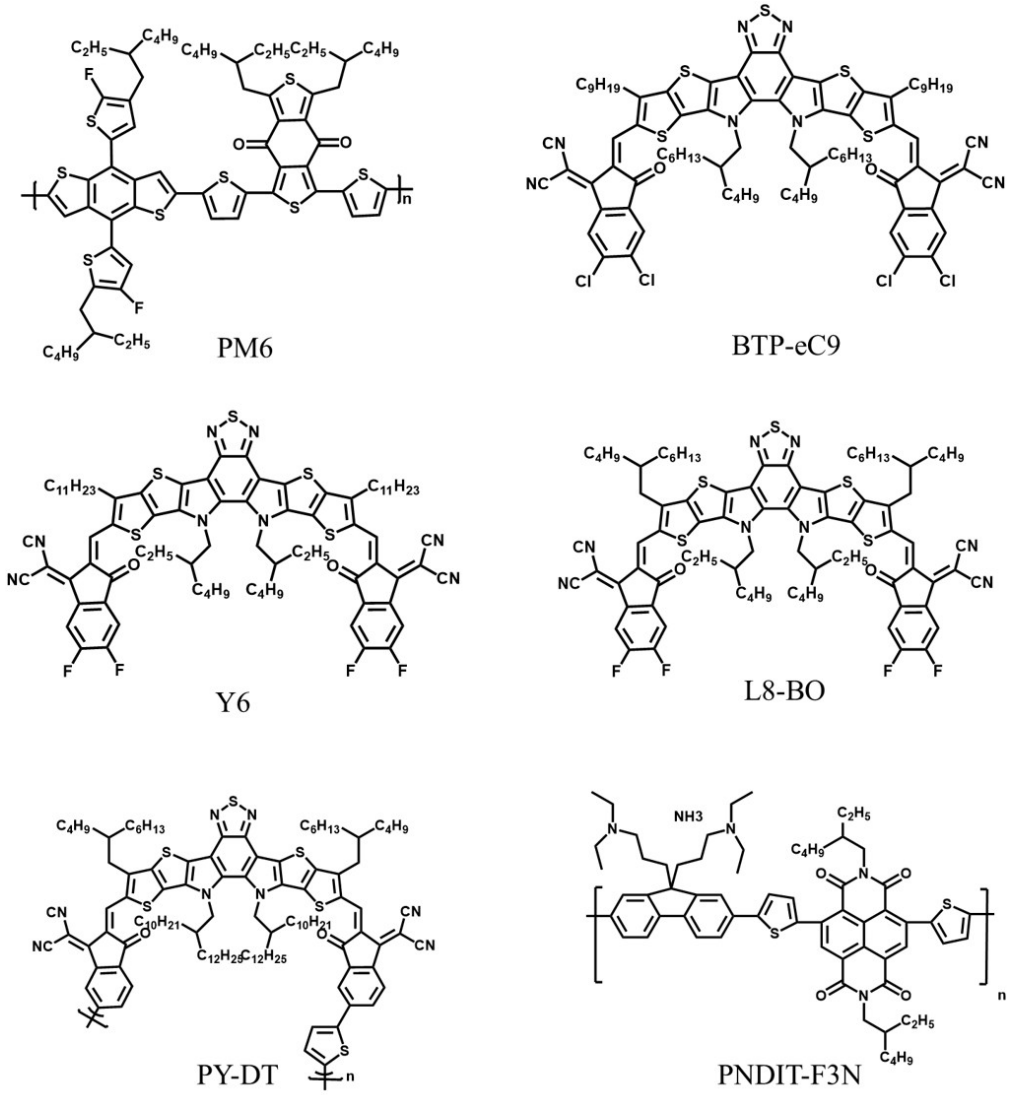

Supplementary Figure 16. All donor, acceptors and ETL structures.

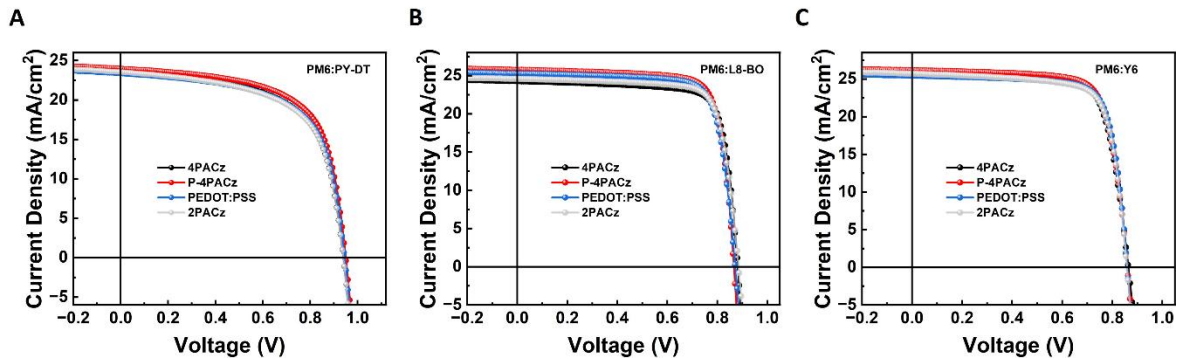

Supplementary Figure 17. A-C: *J–V* curves of PM6:PY-DT, PM6:L8-BO, and PM6:Y6 devices with HTLs.

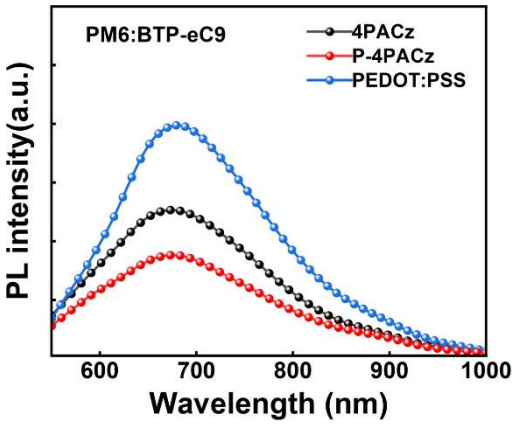

Supplementary Figure 18. PL emission of PM6:BTP-eC9 neat film with 4PACz, P-4PACz and PEDOT:PSS under 565 nm excitation.

Supplementary Table 1. Summary of contact angle calculation results.

Films	Θ_{FA} (°)	Θ_{WATER} (°)	γ^d (mN/m)	γ^p (mN/m)	γ (mN/m)	**Ref.**
ITO	54.0	48.0	40.1	14.9	55.0	
ITO/PEDOT:PSS	6.0	8.0	39.9	36.8	76.7	
ITO/4PACz	61.0	80.0	35.4	5.4	40.8	
ITO/P-4PACz	67.0	86.0	34.0	4.0	38.0	
PM6:BTP-eC9 (1:1.2)	102.7	60.1	28.7	0.2	28.9	[1]

Supplementary Table 2. Devices based on P-4PACz HTL with different solution concentrations.

Hole Transporting Layer	V_{OC} **(V)**	J_{SC} **(mA/cm^2)**	**FF (%)**	**PCE (%)**
PEDOT:PSS	0.85	25.81	77.19	17.04

0.2mg/ml P-4PACz	0.86	26.07	75.95	17.02
0.3mg/ml P-4PACz	0.86	26.39	77.41	18.39
0.4mg/ml P-4PACz	0.87	25.77	77.23	17.95
0.5mg/ml P-4PACz	0.86	26.52	76.66	18.29

Supplementary Table 3. Performance parameters (V_{OC}, J_{SC}, J_{EQE}, FF, and PCE) of champion PM6:BTP-eC9 OSCs with various hole transport layers.

Hole Transporting Layer	V_{OC} (V)	J_{SC} (mA/cm^2)	J_{EQE} (mA/cm^2)	FF (%)	PCE (%)
4PACz	0.865	27.421	25.904	76.54	18.28
P-4PACz	0.866	27.872	26.452	78.86	19.03
PEDOT:PSS	0.859	26.952	25.129	78.81	18.22

Supplementary Table 4. Performance parameters (V_{OC}, J_{SC}, FF, and PCE) of champion PM6:Y6 OSCs with various hole transport layers.

Hole Transporting Layer	V_{OC} (V)	J_{SC} (mA/cm^2)	FF (%)	PCE (%)
4PACz	0.8641	25.8403	72.61	16.21
P-4PACz	0.8602	26.1617	74.35	16.73
PEDOT:PSS	0.8596	25.4314	74.69	16.32
2PACz	0.8587	25.7308	73.51	16.24

Supplementary Table 5. Performance parameters (V_{OC}, J_{SC}, FF, and PCE) of champion PM6: PY-DT OSCs with various hole transport layers.

Hole Transporting Layer	V_{OC} (V)	J_{SC} (mA/cm^2)	FF (%)	PCE (%)
4PACz	0.9394	23.8707	68.71	15.40
P-4PACz	0.9503	23.9253	71.92	16.35
PEDOT:PSS	0.9459	23.3757	71.47	15.79
2PACz	0.9386	23.7043	70.18	15.61

Supplementary Table 6. Performance parameters (V_{OC}, J_{SC}, FF, and PCE) of champion PM6: L8-BO OSCs with various hole transport layers.

Hole Transporting Layer	V_{OC} (V)	J_{SC} (mA/cm^2)	FF (%)	PCE (%)
4PACz	0.8818	25.2651	78.26	17.44
P-4PACz	0.8696	26.4909	78.58	18.16
PEDOT:PSS	0.8718	26.2946	77.73	17.82
2PACz	0.885	25.6213	77.9	17.66

REFERENCES

1. Chen, S.; Zhu, S.; Hong, L.; et al. Binary Organic Solar Cells with over 19 % Efficiency and Enhanced Morphology Stability Enabled by Asymmetric Acceptors. *Angew. Chem. Int. Ed.* **2024**, *63*. https://dx.doi.org/10.1002/anie.202318756.